

normally prolific ($d, p\gamma$) reactions will generally be less successful in the $f_{7/2}$ shell than they have been in the $1p$, $2s$, and $1d$ shells in establishing spin properties of odd- A nuclei.

ACKNOWLEDGMENT

The Yale authors wish to thank Dr. D. E. Alburger for extending to them the hospitality of the Brookhaven Laboratory.

Studies on the $\text{Ne}^{22}(d, p\gamma)\text{Ne}^{23}$ Reaction*

A. J. HOWARD,[†] J. P. ALLEN,[‡] AND D. A. BROMLEY

Nuclear Structure Laboratory, Yale University, New Haven, Connecticut

AND

J. W. OLNESS AND E. K. WARBURTON

Brookhaven National Laboratory, Upton, New York

(Received 7 October 1966)

States of Ne^{23} below 4 MeV in excitation energy have been studied via the $\text{Ne}^{22}(d, p\gamma)\text{Ne}^{23}$ reaction. De-excitation branching ratios for these states were determined by two-parameter analysis of proton-gamma coincidence spectra observed at a bombarding energy $E_d=3.40$ MeV. Proton-gamma angular correlations were measured in a collinear geometry at $E_d=2.72$ and 3.52 MeV in order to obtain information on possible spin assignments for the 1.70-, 1.83-, and 2.31-MeV states. Assuming the most probable value of $J=\frac{5}{2}$ for the Ne^{23} ground state, these results indicate $J=\frac{3}{2}$ or $\frac{7}{2}$ for the 1.70-MeV state and $J=\frac{3}{2}$ for the 1.83-MeV state. A gamma-gamma angular correlation was also studied at $E_d=2.85$ MeV, leading, when combined with previous information, to the assignment $J^\pi=\frac{3}{2}^-$ for the 3.22-MeV state. Presently available evidence on the states of Ne^{23} is shown to be consistent in general with the predictions of a strong-coupling collective model; tentative assignments of members of Nilsson rotational bands are presented for these states.

I. INTRODUCTION

THOUGH Ne^{23} is a nuclear system lying in the midst of a most heavily studied region of the $2s$ - $1d$ nuclear shell, to date only a limited amount of information is available concerning the properties of this system. Previously presented information concerning the static properties of Ne^{23} was derived primarily from particle studies on the $\text{Ne}^{22}(d, p)\text{Ne}^{23}$ reaction.^{1,2} Freeman¹ established the excitation energies associated with 17 excited states in Ne^{23} below $E_x=5.23$ MeV; neon gas either of natural isotopic composition (90.8% Ne^{20} , 0.26% Ne^{21} , 8.9% Ne^{22}) or enriched to 59% Ne^{22} formed the targets, deuteron beams in the energy range $E_d=4.75$ -7.50 MeV were employed, and the proton groups were analyzed with a broad-range magnetic spectrograph situated at 90° to the beam. Pullen, Sperduto, and Kashy² have more recently measured the angular distributions of proton groups associated with formation of Ne^{23} states below 4.0-MeV excitation energy. Stripping characteristics were observed in the formation of seven of these (ten) states, and the neutron

orbital angular momentum transfer numbers were assigned from conventional distorted-wave Born-approximation (DWBA) analyses.

Two observations on the dynamic properties associated with the excited states of Ne^{23} have been reported previously: (1) Proton-gamma coincidence measurements on the $\text{Na}^{23}(n, p\gamma)\text{Ne}^{23}$ reaction carried out by Bass and Saleh³ establish the origin of eight gamma-ray transitions connecting Ne^{23} states below 4.0-MeV excitation energy. (2) The half-life of the $\frac{1}{2}^+$, 1.02-MeV (first-excited) Ne^{23} state has been most recently determined by Fossan, McDonald, and Chase⁴ to be $(1.78 \pm 0.10) \times 10^{-10}$ sec.

The present study of Ne^{23} entails three distinctly different experimental investigations of the $\text{Ne}^{22}(d, p\gamma)\text{Ne}^{23}$ reaction. The first study, reported in Sec. IIA, was designed to establish gamma-ray branching ratios for states of Ne^{23} through two-parameter analyses of proton-gamma coincidence spectra. A bombarding energy of $E_d=3.40$ MeV was used in this work. The second study, reported in Sec. IIB, was intended to obtain information on the spins of the lower lying Ne^{23} states and also on the multipole amplitude ratios of the associated gamma-ray transitions. For this purpose, proton-gamma angular correlation measurements were carried out at $E_d=2.72$ MeV and also at $E_d=3.52$ MeV

* Work supported in part by the U. S. Atomic Energy Commission.

[†] On leave of absence (1966-67) from Trinity College, Hartford, Connecticut.

[‡] Present address: Physics Department, University of Washington, Seattle, Washington.

¹ J. M. Freeman, Phys. Rev. **120**, 1436 (1960).

² D. J. Pullen, A. Sperduto, and E. Kashy, Bull. Am. Phys. Soc. **10**, 38 (1965); D. J. Pullen (private communication).

³ R. Bass and F. M. Saleh (private communication).

⁴ D. B. Fossan, R. E. McDonald, and L. F. Chase, Jr., Phys. Rev. **141**, 1018 (1966).

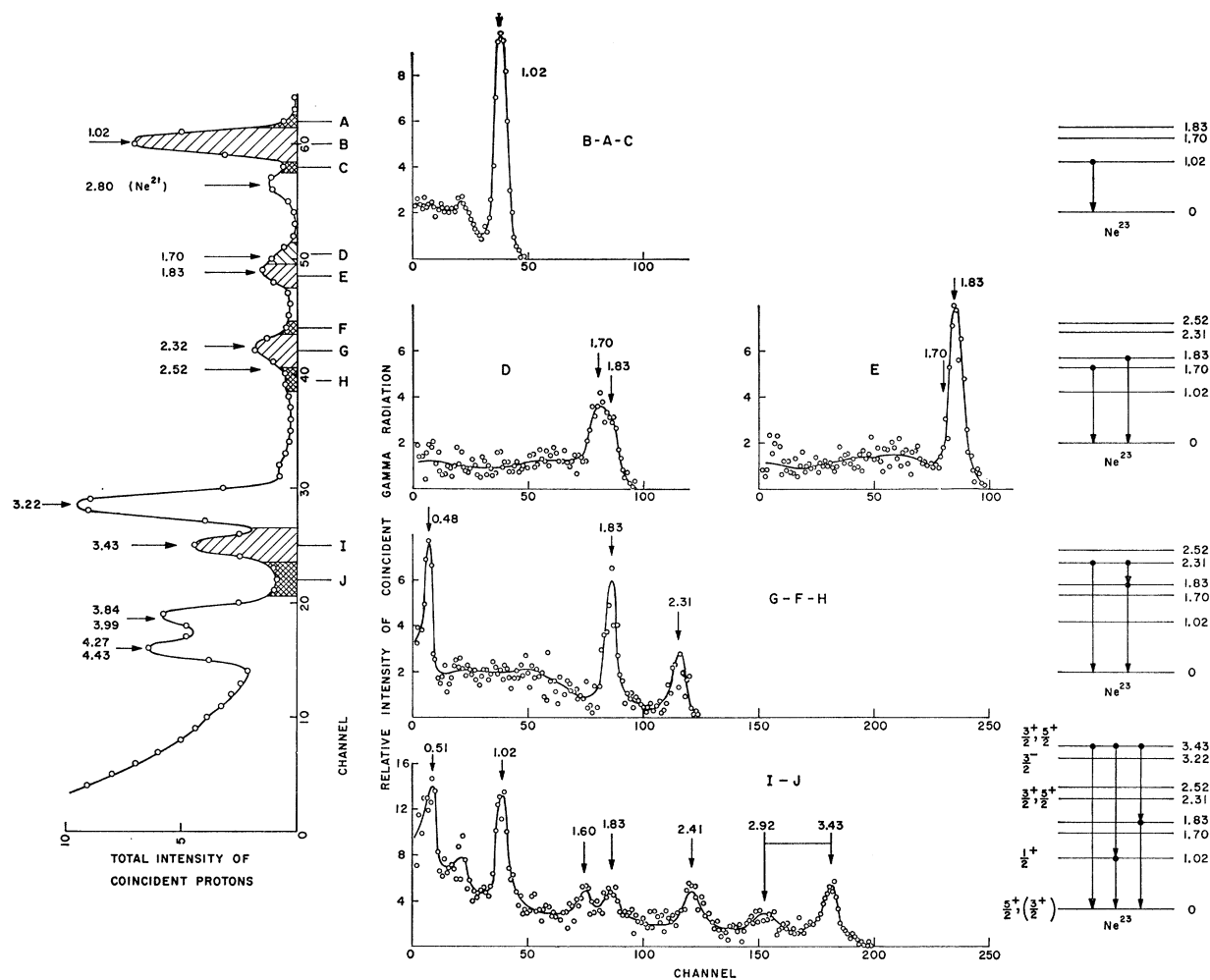


FIG. 1. Gamma-ray spectra observed in coincidence with selected regions of the proton spectrum in the $\text{Ne}^{22}(d, p\gamma)\text{Ne}^{23}$ reaction at $E_d=3.40$ MeV, $\theta_\gamma=45^\circ$, and $\theta_p=90^\circ$. The proton groups observed to be in coincidence with gamma radiation in the energy range 0 to 4 MeV are displayed in the left section of the figure; here the numeric labels identify the proton groups according to their excitation energy (MeV) in Ne^{23} , and the alphabetic labels refer to specific foreground (shaded) or background (cross-hatched) regions of the proton spectrum. The gamma rays observed to be coincident with selected "foreground-only" regions of the proton spectrum are displayed in the center section of the figure; here alphabetic labels correspond to those indicated in the coincident proton spectrum, and the numeric labels identify observed gamma-ray transition energies (MeV). These transitions are positioned in the Ne^{23} level schemes presented in the right section of the figure.

in a collinear geometry⁵ ($\theta_p \simeq 180^\circ$). Thirdly, a $\gamma\text{-}\gamma$ correlation measurement, described in Sec. IIC, was undertaken in order to investigate the spin of the 3.22-MeV Ne^{23} state. Presently available spectroscopic information on Ne^{23} states below 4-MeV excitation energy is summarized in Sec. III, and a tentative interpretation of this information is then given in Sec. IV.

II. EXPERIMENTAL DETERMINATIONS

A. Gamma-Ray Branching-Ratio Measurements

Deuteron beams from the Brookhaven National Laboratory 3-MeV Van de Graaff accelerator were

⁵ A. E. Litherland and A. J. Ferguson, *Can. J. Phys.* **39**, 778 (1961).

employed for all of the measurements reported herein. The gaseous target⁶ used for this particular study was of isotopic constitution 92.7% Ne^{22} , 0.2% Ne^{21} , and 7.1% Ne^{20} ; an upper limit of 0.5% nitrogen impurity was ascertained by mass spectrometer analyses, and no other contaminants ($\leq 0.01\%$) were detected in this target gas.

Details of the gas target chamber used here have been described elsewhere.⁷ Briefly, deuterons of energy $E_d=3.40$ MeV were incident upon a 0.1-mil thick nickel entrance window; degraded by ~ 200 keV, the beam entered the target gas itself, which was at 10 cm of

⁶ A. J. Howard and W. W. Watson, *J. Chem. Phys.* **40**, 1409 (1964).

⁷ A. J. Howard, D. A. Bromley, and E. K. Warburton, *Phys. Rev.* **137**, B32 (1965).

mercury absolute pressure and had 3 cm longitudinal extent. Charged particles originating from the gaseous reaction volume were observed by a conventional 0.25-cm² solid-state detector, which was immersed within the target gas and was located at an angle $\theta_p=90^\circ$ to the deuteron beam axis at a distance of 5 cm from the center of the reaction volume. A tantalum collimator located between the reaction volume and the charged particle detector confined the angular divergence in θ_p to $\pm 10^\circ$ and also occluded the entrance window as well as the tantalum beam stop from the direct view of the charged-particle detector.

The ground-state Q values of the $\text{Ne}^{22}(d, p)\text{Ne}^{23}$ and $\text{Ne}^{22}(d, \alpha)\text{F}^{20}$ reactions are $Q_m=+2.968$ MeV and $+2.699$ MeV, respectively.⁸ Consequently, a 0.5-mil thick aluminum absorber foil was employed to remove all alpha-particle groups associated with the (d, α) reaction from the observed charged particle spectrum; proton groups corresponding to formation of known Ne^{23} states up to and inclusive of the 4.43-MeV state and also deuterons elastically scattered from the target gas were passed by this absorber.

Gamma radiations were examined by means of a 5×5-in. NaI (Tl) detector placed external to the gas chamber at $\theta_\gamma=45^\circ$ to the deuteron beam axis. The front face of this detector was situated 5 cm from the "effective" reaction volume, which represented the reaction volume directly observed by the charged-particle detector.

Proton-gamma coincidences were analyzed by a TMC 16384-channel pulse-height analyzer operating in a 256(gamma)×64(proton)-channel mode. Coincidence conditions were imposed by an external circuit of 60 nsec resolving time. Data were acquired over a period of 23 h at a beam current of 6 nA. At this beam current, the ratio of real-to-random coincidence events was measured to be $\sim 25:1$. The data so obtained were recorded on magnetic tape for later analyses with an IBM 7094 computer. The methods of analysis, as applied to the two-parameter spectra, have previously been described in detail.⁹ The general procedure used to determine the gamma spectrum coincident with a given proton group is illustrated for several cases in Fig. 1.

The (gamma ray) geometry employed for this single measurement, characterized by $\theta_\gamma=45^\circ$ and $h=5$ cm, was advantageous in the respect that the effects of possible angular correlations on the measured branching ratios were minimized. These effects were subsequently estimated to be negligible. The principal disadvantage resulting from this close geometry was the enhancement of sum-peak contributions in the measured gamma-ray spectra, and careful considerations of this effect were included in the spectral analyses. Gamma-ray intensi-

TABLE I. Gamma-ray branching ratios (BR) in Ne^{23} observed in the present studies.

E_i (MeV)	E_f (MeV)	BR (%)	E_i (MeV)	E_f (MeV)	BR (%)	
3.99	0	56±6	3.22	0	18±2	
	1.02	<7		1.02	82±2	
	1.70	8±8		1.70	<4	
	1.83	<5		1.83	<4	
	2.31	36±8		2.31	<5	
	2.52	<4		2.52	<5	
	3.22	<7				
	3.43	<10		2.52	0	<35
	3.84	<4			1.02	<25
					1.70	100
3.84	0	2±2	2.31	1.83	<30	
	1.02	57±6		2.31	<30	
	1.70	<8				
	1.83	41±6		1.83	0	45±2
	2.31	<6			1.02	10±2
	2.52	<6			1.70	<7
	3.22	<3			1.83	45±2
	3.43	<4				
3.43	0	54±4	1.70	0	100	
	1.02	32±6		1.02	<5	
	1.70	<2		1.70	<4	
	1.83	14±3		0	100	
	2.31	<9			1.02	<5
	2.52	<3				
	3.22	<3				
	3.22	<5				

ties, and also sum-peak contributions, were computed from previously available data for 5×5-in. NaI (Tl) detectors.¹⁰ The results are summarized in Table I, which gives the gamma-ray branching ratios determined from the present experiment. The branching ratios quoted for the 1.70-, 1.83-, and 2.31-MeV Ne^{23} states incorporate additional data obtained from the correlation measurements of Sec. IIB, for which cases the counting statistics were markedly superior. As a final consideration, possible ambiguities associated with the 7.1% Ne^{20} (and 0.2% Ne^{21}) isotopic impurities in the target gas were ruled out by inspection of the results of similar measurements performed with a gas target of 99.8% Ne^{20} constitution.

B. Proton-Gamma Angular-Correlation Measurements

Proton-gamma angular correlations in the $\text{Ne}^{22}(d, p\gamma)\text{Ne}^{23}$ reaction were measured utilizing a collinear geometry with protons detected in an annular counter located at $\theta_p=180^\circ$ relative to the incident deuteron beam. The target for these measurements was a cylindrical cell of 99.9% Ne^{22} gas located at the center of a scattering chamber which has been described in detail previously.⁹ The cell consisted of a 2-cm long section of 0.65-cm diam brass tubing (0.1-mm wall thickness) placed with its axis coincident with the beam axis. The ends of the cell were of 0.04-mil nickel foil, which confined the gas at a pressure of 30-cm Hg absolute and

⁸ *Nuclear Data Sheets*, compiled by K. Way et al. (Printing and Publishing Office, National Academy of Science—National Research Council, Washington 25, D. C.).

⁹ J. W. Olness and E. K. Warburton, *Phys. Rev.* **151**, 792 (1966).

¹⁰ S. H. Vegors, L. L. Marsden, and R. L. Heath, Phillips Petroleum Company Report No. IDO-16370, 1958 (unpublished); F. C. Young, H. T. Heaton, G. W. Phillips, P. D. Forsyth, and J. B. Marion, *Nucl. Instr. Methods* **44**, 109 (1966).

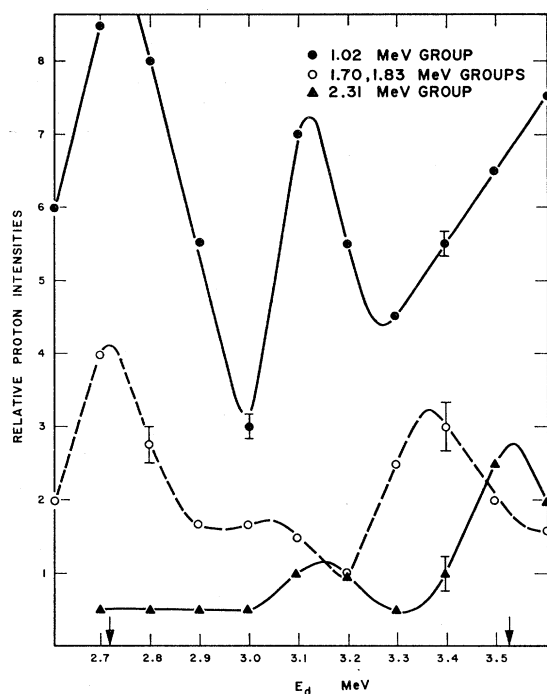


FIG. 2. Relative intensities of Ne^{23} proton groups observed at $\theta_p = (165 \pm 6)^\circ$ as a function of the deuteron bombardment energy when employing a 0.04-mil thick nickel entrance window. Arrows on the abscissa indicate the two energies selected for the present proton-gamma angular-correlation measurements.

resulted in an energy loss for the incident deuteron beam of < 100 keV per foil. Charged particles emanating from the gaseous reaction volume were detected at $\theta_p \approx (165 \pm 6)^\circ$ by an annular detector⁹ of $\sim 1.0\text{-cm}^2$ active area located external to the gas cell itself. The detector also viewed events which originated in the nickel entrance and exit windows. Deuterons scattered from these foils as well as those scattered from the gas were stopped by an appropriately placed (annular) aluminum absorber foil of 2-mil thickness; all alpha-particle groups associated with the $\text{Ne}^{22}(d, \alpha)\text{F}^{20}$ reaction

were also stopped by this absorber. Gamma rays were measured by a $5 \times 5\text{-in.}$ NaI (TI) detector placed with its front face 16 cm from the target volume.

The intensities of proton groups corresponding to formation of the 1.02-, 1.70-, 1.83-, and 2.31-MeV Ne^{23} states were determined as a function of deuteron bombardment energy in the interval $E_d = 2.5$ to 3.6 MeV. As demonstrated in Fig. 2, the maximum intensities for the (unresolved) 1.70- and 1.83-MeV Ne^{23} proton groups and for the 2.31-MeV Ne^{23} proton group occurred at $E_d = 2.72$ MeV and 3.52 MeV, respectively. Consequently, angular correlation measurements were carried out at each of these two bombardment energies.

Proton-gamma coincidence spectra were measured with the TMC 16384-channel analyzer, as described in Sec. IIA, for gamma-ray detection angles $\theta_\gamma = 0, 30, 45, 60,$ and 90° . The 0, 45, and 90° measurements were repeated as a check on reproducibility. Beam currents of 4 nA were used in these studies, which resulted in a ratio of real-to-random coincidences of about 20:1. The elapsed time for each correlation point measurement was 2.0 and 4.0 h for the respective $E_d = 2.72\text{-}$ and 3.52-MeV studies.

The procedures of analyses described in Sec. IIA were used to determine, for each angle θ_γ , the intensities of the various de-excitation gamma-rays coincident with each proton group. Having thus obtained the experimental correlation data from the two-parameter arrays, the method of least squares was applied to fit the correlation data, for each of the two bombardment energies used, with the following two Legendre-polynomial expansions:

$$W(\theta) = a_0 + a_2 P_2(\cos\theta), \quad (1)$$

and

$$W(\theta) = a_0 + a_2 P_2(\cos\theta) + a_4 P_4(\cos\theta). \quad (2)$$

The goodness of fit so obtained is expressed in the usual χ^2 presentation,^{9,11} wherein the expectation value of χ^2 is unity. Table II presents the values of a_2/a_0 and a_4/a_0 obtained from the fits to Eqs. (1) and (2), respectively.

For the two proton-gamma correlations involving the

TABLE II. Results of Legendre-polynomial least-squares fits to gamma-ray angular distributions in Ne^{23} .

E_d (MeV)	E_i (MeV)	E_f (MeV)	a_2/a_0	a_4/a_0	$\chi^2(a_2)$	$\chi^2(a_4)$
2.72	1.02	0	$-(0.01 \pm 0.01)$		1.9	
3.52	1.02	0	$-(0.005 \pm 0.008)$		2.8	
2.72	1.70	0	$-(0.58 \pm 0.04)$	$+(0.07 \pm 0.04)$	2.7	2.7
3.52	1.70	0	$-(0.39 \pm 0.06)$	$+(0.02 \pm 0.06)$	0.5	0.7
SUM	1.70	0	$-(0.56 \pm 0.05)$	$+(0.06 \pm 0.05)$	1.3	1.3
2.72	1.83	0	$-(0.04 \pm 0.02)$	$-(0.02 \pm 0.02)$	0.8	0.6
3.52	1.83	0	$-(0.22 \pm 0.03)$	$+(0.02 \pm 0.03)$	0.9	1.0
SUM	1.83	0	$-(0.13 \pm 0.02)$	$-(0.002 \pm 0.02)$	0.2	0.2
3.52	2.31	0	$+(0.66 \pm 0.04)$	$+(0.07 \pm 0.04)$	1.8	1.5
3.52	2.31	1.02	$+(0.29 \pm 0.15)$	$+(0.30 \pm 0.20)$	1.1	0.4
3.52	2.31	1.83	$-(0.30 \pm 0.03)$	$-(0.01 \pm 0.04)$	1.1	1.6
3.52	1.83 ^a	0	$-(0.01 \pm 0.05)$	$+(0.03 \pm 0.06)$	1.0	1.5

^a 2.31 \rightarrow 1.83 \rightarrow 0; 2.31 \rightarrow 1.83 unobserved.

¹¹ A. R. Poletti and E. K. Warburton, Phys. Rev. **137**, B595 (1965).

1.02-MeV Ne^{23} state, fits were obtained by Eq. (1) only: Previous studies^{2,12,13} have established the spin and parity for the 1.02-MeV Ne^{23} state as $J^\pi = \frac{1}{2}^+$, and therefore the relevant proton-gamma angular correlation is anticipated to be isotropic. The intensity of the 1.02-MeV gamma-ray photopeak was obtained to within 1.8% and 1.2% statistical accuracy for each correlation point in the respective $E_d = 2.72$ - and 3.52-MeV studies. Thus the results as presented in Table II concerning these observed correlations provided empirical information for estimating the magnitude of the systematic errors involved in the experiment and subsequent analytical procedures. In each of these two sets of correlation data, the systematic errors so estimated were $\sim 1\%$ in magnitude. In all of the other experimental correlations considered below, statistical uncertainties were in excess of 3% and were considered to represent the dominant source of uncertainty in the associated results. In cases where a given correlation was measured at each of the two bombardment energies, the data sets were summed to obtain a "summed" correlation which was subsequently fitted in the fashion outlined above.

The next stage in the analyses involved fitting the experimental correlation data with pertinent theoretical correlation functions.¹¹ In the $\text{Ne}^{22}(d, p)\text{Ne}^{23}$ reaction, Method II geometry⁵ restricts populated Ne^{23} magnetic substates relative to the beam axis to be either $\frac{1}{2}$ or $\frac{3}{2}$ in magnitude; in the absence of polarization sensitivity, as in the present experimental situation, the substate population parameters, $P(a)$, are further restricted in that $P(-\frac{3}{2}) = P(+\frac{3}{2})$ and $P(-\frac{1}{2}) = P(+\frac{1}{2})$. The finite deviation from ideal collinear geometry present in the experimental situation employed allowed relatively small, fast-convergent populations of sequentially higher (if J -allowed) magnetic substates: Population of magnitude $\frac{5}{2}$ magnetic substates were conservatively considered to be $\leq 10\%$ of the maximum of $P(\frac{1}{2})$ or $P(\frac{3}{2})$ populations,^{5,9} and higher substate populations were neglected in the ensuing analyses.

The theoretical angular correlations were fitted to the data by the procedures discussed in detail previously.^{9,11} The population parameters discussed above are employed as variables in obtaining best fits (i.e., minima in χ^2) to single experimental correlations by the linear method of least squares for selected spin sequences and *discrete* values of the multipole amplitude ratio x .¹⁴ For each spin sequence considered, best fits were obtained for values of arc tangent x equal to -90° , -85° , -80° , \dots , $+90^\circ$, and hence the goodness of fit χ^2 of the theoretical angular correlation expressions to the experi-

¹² H. B. Burrows, T. S. Green, S. Hinds, and R. Middleton, Proc. Phys. Soc. (London) **A69**, 310 (1956).

¹³ J. P. Allen, Ph.D. dissertation, Yale University, 1965 (unpublished).

¹⁴ Here $x = \langle b || L+1 || a \rangle / \langle b || L || a \rangle$, where a and b represent the respective initial and final states for the gamma-ray transition, and L is the lowest order multipolarity therefore allowed; the Litherland-Ferguson sign convention for $M(L)/E(L+1)$ mixtures is employed.

Table III. Multipole amplitude ratios for Ne^{23} gamma-ray transitions as observed in the present studies.

E_i (MeV)	E_f (MeV)	J_i	J_f	Multipole amplitude ratio ^a
1.70	0	$\frac{3}{2}$	$\frac{5}{2}$	$-5.7 \leq x \leq -0.38$
1.70	0	$\frac{7}{2}$	$\frac{5}{2}$	$+0.05 \leq x \leq +0.78, +1.2 \leq x \leq +2.6$
1.83	0	$\frac{3}{2}$	$\frac{5}{2}$	$-\infty \leq x \leq +\infty$
2.31	0	$\frac{3}{2}$	$\frac{5}{2}$	$-5.6 \leq x \leq -0.42$
2.31	0	$\frac{5}{2}$	$\frac{5}{2}$	$-0.84 \leq x \leq -0.11$
2.31	1.83	$\frac{3}{2}$	$\frac{3}{2}$	$-8.1 \leq x \leq -2.7, -0.08 \leq x \leq +0.11$
2.31	1.83	$\frac{5}{2}$	$\frac{3}{2}$	$-0.10 \leq x \leq +0.09$

^a Limitations imposed at the 0.1% statistical confidence limit.

mental data is essentially obtained as a function of $\arctan x$. Data concerning a particular proton-gamma correlation observed at each of the two bombardment energies employed were treated in two analytical methods: (1) The two sets of correlation data were summed and then fitted ("summed fit"). (2) The two correlations were individually fitted and then a combined χ^2 analysis was generated from these two fits ("combined fit"). Similar procedures were subsequently employed, where appropriate, in simultaneously fitting two or three dependent correlations. All but one of the involved multipole amplitude ratios were fixed in these multiple correlation analyses via considerations of the previous single-correlation results, the goodness of fit being obtained as a function of the remaining (unfixed) multipole amplitude ratio. Concomitant spin and multipole amplitude ratio determinations resulting from these studies are presented in the ensuing subsections and are summarized in Table III.

1. The 1.70-MeV State

No information has previously been reported concerning the spin (and parity) of the 1.70-MeV Ne^{23} state. The present studies demonstrate that the predominant mode ($\geq 95\%$ relative intensity) of decay for this state is the direct transition to the Ne^{23} ground state, for which previous evidence^{2,4,8} strongly indicates a $J^\pi = \frac{5}{2}^+$ assignment. In theoretical analyses of the proton-gamma angular correlation involving the $1.70 \rightarrow 0$ Ne^{23} gamma-ray transition, half-integral spin assignments from $J = \frac{1}{2}$ through $J = 11/2$ were considered for the 1.70-MeV state together with a $J = \frac{5}{2}$ assignment for the Ne^{23} ground state: As concerns the 1.70-MeV state, $J \geq 13/2$ assignments can reasonably be eliminated from further consideration by the observed 1.70-MeV Ne^{23} state lifetime limitation imposed by the coincidence circuitry resolving time, $\lesssim 6 \times 10^{-8}$ sec. The $J = \frac{5}{2}$ assignment for the Ne^{23} ground state is discussed further in Sec. III and is assumed in the remainder of this section. Ruling against spin assignments at the 0.1% statistical confidence limit, theoretical analyses of the pertinent $E_d = 2.72$ -MeV correlation allowed only $J = \frac{3}{2}$ or $\frac{7}{2}$ for the 1.70-MeV Ne^{23} state, and analyses of the $E_d = 3.52$ -MeV data sanctioned $J = \frac{3}{2}$,

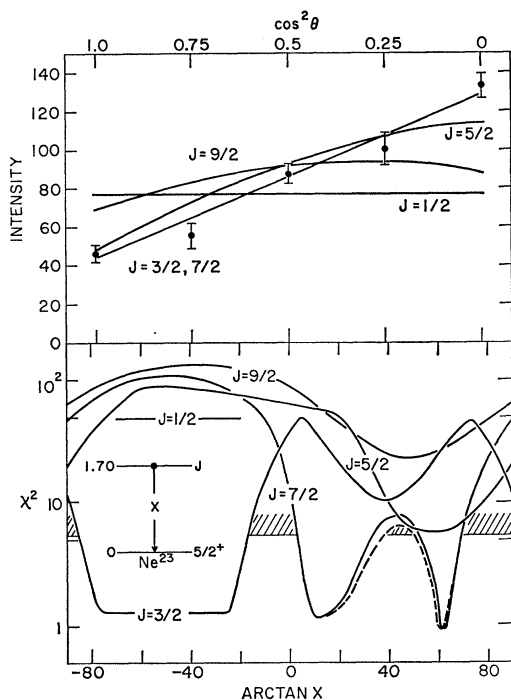


FIG. 3. Summed correlation results for the $1.70 \rightarrow 0$ transition. The upper portion of the figure displays the sum of the data for the two sets of correlation data obtained on the $1.70 \rightarrow 0$ transition, and the lower portion illustrates χ^2 as a function of $\arctan x$ for $J = \frac{1}{2}$ through $\frac{9}{2}$ assignments to the 1.70-MeV state. In the lower portion, the line below the shaded region represents the 0.1% statistical confidence limit, and the dashed curve represents the fit obtained by including the estimated maximum finite size effect in the fitting procedure. The curves in the upper portion correspond to the best fits (i.e., those fits associated with minima in χ^2) of the theoretical correlation functions to the observed correlation.

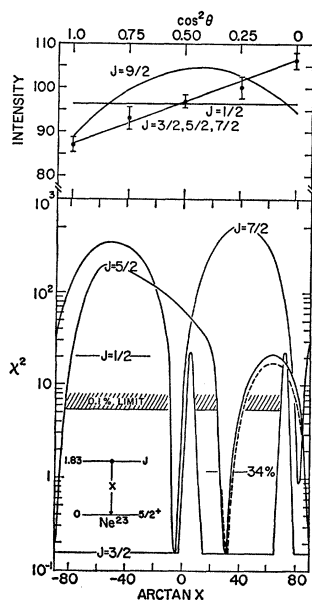


FIG. 4. Summed correlation results for the $1.83 \rightarrow 0$ transition. The upper portion of the figure displays the sum of the two sets of correlation data on the $1.83 \rightarrow 0$ transition obtained at $E_d = 2.72$ and 3.52 MeV. The lower portion illustrates χ^2 as a function of $\arctan x$ for $J = \frac{1}{2}$ through $\frac{9}{2}$ assignments to the 1.83-MeV state. The 0.1% and 34% statistical confidence limits are indicated, and the dashed curve represents the fit obtained by including the estimated maximum finite size effect in the fitting procedure. The curves in the upper portion correspond to the best fits of the theoretical correlation functions to the observed correlations.

$\frac{5}{2}$, or $\frac{7}{2}$ for this state; both summed (see Fig. 3) and combined fits to these data permitted only $J = \frac{3}{2}$ or $\frac{7}{2}$ assignments. It is therefore concluded that $J = \frac{3}{2}$ or $\frac{7}{2}$ are allowed by these data for the 1.70-MeV Ne^{23} state; associated delimitations on the multipole amplitude ratio for the $1.70 \rightarrow 0$ Ne^{23} transition are presented in Table III.

2. The 1.83-MeV State

Analogous to the 1.70-MeV state situation, no information on the spin (and parity) of the 1.83-MeV Ne^{23} state has previously been reported. The level in question is observed to decay predominantly ($\geq 95\%$) to the ground state, and half-integral J assignments of $\frac{1}{2}$ through $11/2$ to this state were considered in the correlation analyses. While analyses of each of the two sets of correlation data observed at $E_d = 2.72$ and 3.52 MeV and also the summed fit (see Fig. 4) allowed

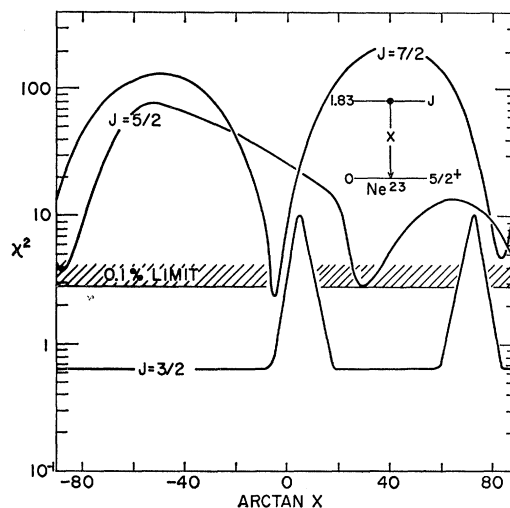


FIG. 5. Combined correlation results for the $1.83 \rightarrow 0$ transition. The combined fit shown is generated from the individual fits to two sets of correlation data obtained for the $1.83 \rightarrow 0$ transition. The 0.1% statistical confidence limit is indicated, and the minimum value of χ^2 for the $J = \frac{3}{2}$ case is located just at the 1% limit (not illustrated). Corrections for the finite-size effect were included, where appropriate, in generating this fit.

$J = \frac{3}{2}$, $\frac{5}{2}$, or $\frac{7}{2}$ assignments for the 1.83-MeV state, the combined fit demonstrated in Fig. 5 ruled against either $J = \frac{5}{2}$ or $\frac{7}{2}$ with $>99\%$ confidence. The reason the combined fit rules out $J = \frac{5}{2}$ or $\frac{7}{2}$ while the individual and summed fits do not is due to the fact that for these two possibilities, the mixing ratio restrictions determined at the two different bombarding energies are not in agreement with one another. This is consistent with expectations for a $J = \frac{3}{2}$ assignment when the $P(\frac{3}{2})/P(\frac{1}{2})$ ratios at the two bombarding energies are different. On the basis of this combined fit, it was concluded with $>99\%$ statistical confidence that $J = \frac{3}{2}$ for the 1.83-MeV Ne^{23} state.

3. The 2.31-MeV State

Neutron orbital angular momentum $l_n=2$ stripping characteristics have been observed by Pullen, Spurduto, and Kashy² in the formation of the 2.31-MeV Ne^{23} state via the (d, p) reaction, which indicates $J^\pi = \frac{3}{2}^+$ or $\frac{5}{2}^+$ for this state. The present studies at $E_d=3.52$ MeV have established that this 2.31-MeV state de-excites to the 1.83-, 1.02-, and 0-MeV states with respective relative intensities 45, 10, and 45%. As regards proton-gamma correlations involving the 2.31-MeV state, the $E_d=3.52$ -MeV measurements were statistically superior to the 2.72-MeV measurements by a factor of ~ 4 , and only the former measurements were utilized in the ensuing theoretical correlation fits.

The first step in the theoretical analyses was to fit the correlation involving the $2.31 \rightarrow 0$ transition for assumed half-integral assignments $J = \frac{1}{2}$ through $11/2$ for the 2.31-MeV state. The results, which are partially illustrated in Fig. 6, eliminate only $J = \frac{1}{2}$ and $11/2$ assignments. Similar analyses were attempted on the correlation involving the (relatively weak) $2.31 \rightarrow 1.02$ transition; however, the $\sim 20\%$ statistical uncertainties associated with this measured correlation precluded the possibility of further limiting the 2.31-MeV state spin assignments by this means.

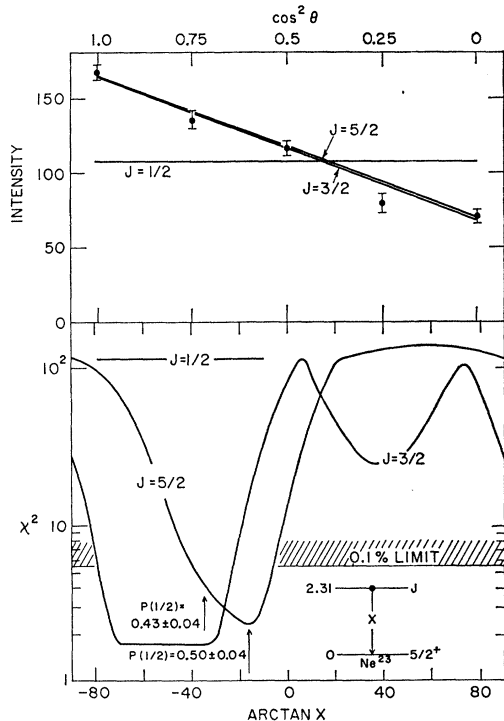


FIG. 6. Correlation results for the $2.31 \rightarrow 0$ transition. The upper portion of the figure displays the data for the correlation data obtained on the $2.31 \rightarrow 0$ transition, and the lower portion illustrates χ^2 as a function of $\arctan x$ for $J = \frac{1}{2}, \frac{3}{2},$ and $\frac{5}{2}$ assignments to the 2.31-MeV state. Values of the population parameter $P(\frac{1}{2})$ determined from the fitting procedure are shown for $x = -0.7$ and -0.3 in the case $J = \frac{3}{2}$ [in the case $J = \frac{5}{2}, P(\frac{1}{2}) < 0.05$ over the entire region of acceptable solutions illustrated].

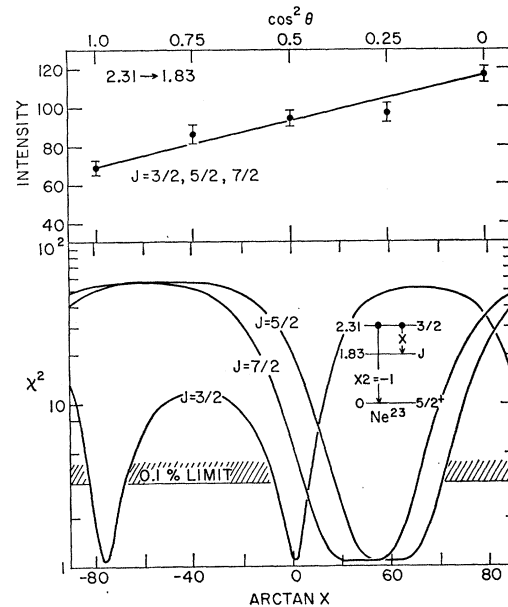


FIG. 7. Two-distribution fit concerning the 2.31-MeV state. The upper portion of the figure displays the experimental correlation data for the $2.31 \rightarrow 1.83$ transition, and the lower portion illustrates χ^2 as a function of $\arctan x$ for simultaneous fits to the $2.31 \rightarrow 0$ and $2.31 \rightarrow 1.83$ distributions under the assumptions presented in the inset energy-level diagram.

The next step was to obtain simultaneous fits to the observed correlations involving the $2.31 \rightarrow 0$ and $2.31 \rightarrow 1.83$ transitions under the following conditions: (1) It was assumed that $J = \frac{3}{2}$ or $\frac{5}{2}$ for the 2.31-MeV state and $J = \frac{3}{2}, \frac{5}{2},$ or $\frac{7}{2}$ for the 1.83-MeV state,¹⁵ (2) the relative population parameters for the 2.31-MeV state consistent with the accepted portions of the above-discussed $2.31 \rightarrow 0$ correlation solutions (see Fig. 6) were effectively specified by selection of one discrete value of the relevant multipole amplitude ratio for each of the two allowed J values (i.e., $\frac{3}{2}$ or $\frac{5}{2}$) for the 2.31-MeV state.¹⁶ In these "two distribution" fits, the multipole amplitude ratio for the $2.31 \rightarrow 1.83$ transition was treated as a variable. The results of these analyses are depicted in Figs. 7 and 8. Of particular interest, either $J = \frac{3}{2}$ or $\frac{5}{2}$ assumed assignments to the 2.31-MeV state were found to produce acceptable solutions with $J = \frac{3}{2}$ (1.83-MeV state) and $J = \frac{5}{2}$ (ground-state) assignments; moreover, all J combinations considered were consistent with the simultaneous fits.

The final step was to generate simultaneous fits to the observed correlations involving the $2.31 \rightarrow 0$ and the

¹⁵ It has previously been concluded herein that $J = \frac{3}{2}$ for the 1.83-MeV state (Sec. II B 2). The present considerations included $J = \frac{5}{2}$ and $\frac{7}{2}$ assignments to the 1.83-MeV state in an attempt to provide a second determination for the spin of this state.

¹⁶ The validity of this step results from the fact that in the present situation, the relative population parameters associated with the theoretical fits change only slightly over the acceptable portions of the χ^2 -versus- x plots displayed in Fig. 6 for each of the $J = \frac{3}{2}$ and $\frac{5}{2}$ cases.

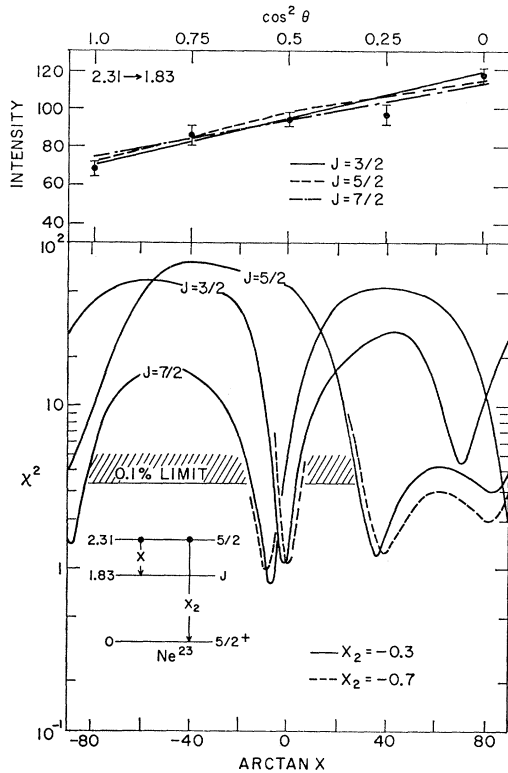


FIG. 8. Two-distribution fit concerning the 2.31-MeV state. The upper portion of the figure displays the correlation data obtained on the 2.31 \rightarrow 1.83 transition, and the lower portion illustrates χ^2 as a function of arctan x for simultaneous fits to the 2.31 \rightarrow 0 and 2.31 \rightarrow 1.83 distributions under the assumptions presented in the inset energy-level diagram.

2.31 \rightarrow 1.83 \rightarrow 0 cascade transitions under the following conditions: (1) It was assumed that $J=3/2$ or $5/2$ for the 2.31-MeV state and $J=3/2$ for the 1.83-MeV state. (2) The relative population parameters for the 2.31-MeV state consistent with the preceding results were specified via the method discussed for the two distribution fits. In these "three distribution" fits, the multipole amplitude ratio for the 1.83 \rightarrow 0 MeV transition was treated as a variable, and the results are illustrated in Fig. 9. Although Fig. 9 indicates that the $J=3/2$ possibility is ruled against with $>90\%$ statistical confidence, the data are judged not to be sufficiently restrictive to warrant rigorous exclusion of this spin possibility; it is concluded that either $J=3/2$ or $5/2$ assignments to the 2.31-MeV state afford acceptable solutions. Limitations on the multipole amplitude ratios associated with the transitions considered in these analyses are contained in Table III.

C. Gamma-Ray Angular-Correlation Measurements

An $l_n=1$ transfer in the formation of the 3.22-MeV state via the $\text{Ne}^{22}(d,p)\text{Ne}^{23}$ reaction has been established in the studies of Pullen, Sperduto, and Kashy²; therefore $J^\pi=1/2^-$ or $3/2^-$ is indicated for this state. In the

studies presented in Sec. IIA, it has been additionally established that the predominant mode ($82\pm 2\%$) of gamma de-excitation of the 3.22-MeV Ne^{23} state is the 2.20-MeV cascade transition to the $1/2^+$, 1.02-MeV state.

Since observation of gamma anisotropy in the angular distribution of gamma radiations originating from any Ne^{23} configuration is sufficient to rule out $J=1/2$ for said state, gamma-ray angular distribution studies were performed on the 2.20-MeV (assumed Ne^{23} 3.22 \rightarrow 1.02) transition observed in the direct gamma-ray spectrum. The gas target material described in Sec. IIB was contained within the target chamber referred to in Sec. IIA. A 3×3 -in. spectrometer was located 12 cm from the target center; pulses therefrom were ultimately stored in a RIDL 400-channel pulse-height analyzer. A second, similar detector (and associated analysis system) was fixed at 90° to the deuteron beam and served as a monitor during the direct gamma-ray angular distribution measurements. The angular distribution of 2.20-MeV radiations was determined at $E_d=2.85$ MeV, a bombardment energy at which the

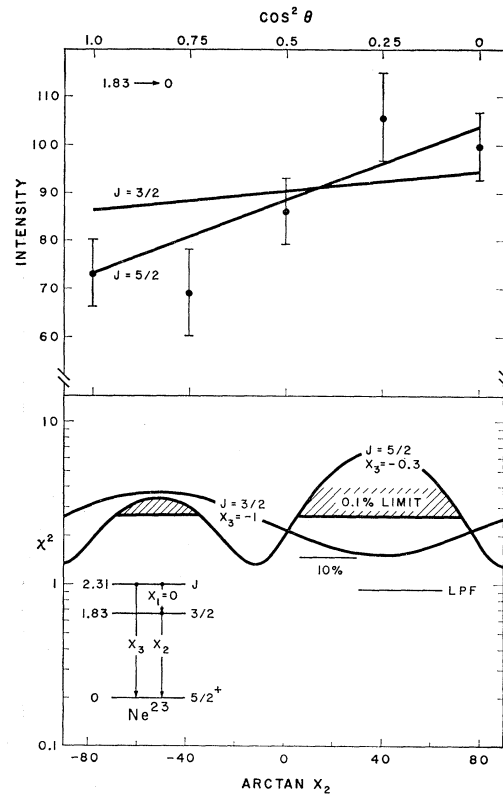


FIG. 9. Three-distribution fit concerning the 2.31-MeV state. The upper portion of the figure displays the correlation data obtained for the cascade 1.83 \rightarrow 0 transition, and the lower portion illustrates χ^2 as a function of arctan x for simultaneous fits to the 2.31 \rightarrow 0, 2.31 \rightarrow 1.83, and 1.83 \rightarrow 0 distributions under the assumptions presented in the inset energy-level diagram and the curve labels. The 0.1% and 10% statistical confidence limits are indicated, and the χ^2 associated with the Legendre polynomial fits to the three distributions is indicated by the line labeled L.P.F.

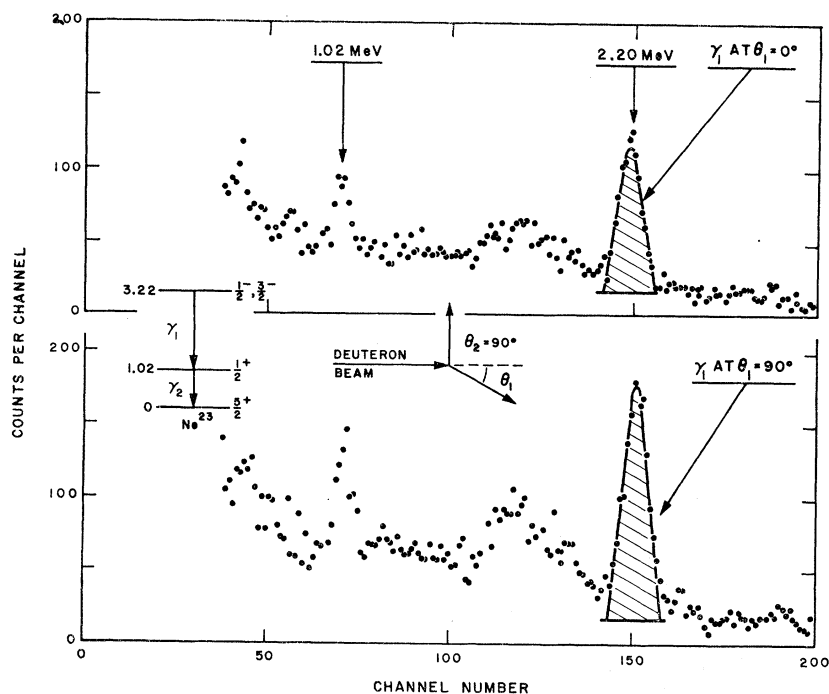


FIG. 10. The gamma-gamma angular-correlation spectra involving the $3.22 \rightarrow 1.02 \rightarrow 0$ cascade as observed in Case-I geometry. Relative intensities are computed from the shaded spectral regions.

2.20-MeV gamma-ray photopeak displayed relative prominence. The angular distribution with respect to the beam axis of 2.20-MeV gamma rays observed at $E_d = 2.85$ MeV is characterized via Eq. (2) by $a_2/a_0 = -(0.37 \pm 0.03)$, $a_4/a_0 = +(0.02 \pm 0.03)$.

In order to eliminate the possibility that a cascade in F^{20} [formed by the $\text{Ne}^{22}(d, \alpha)\text{F}^{20}$ reaction] was responsible for the above-observed anisotropic 2.20-MeV gamma-ray angular distribution, a gamma-gamma angular correlation measurement involving the $3.22 \rightarrow 1.02 \rightarrow 0$ cascade was performed in Litherland-Ferguson Method I geometry⁵: The two gamma-ray spectrometers were located as previously described, and the fast-slow time coincidence circuitry utilized in the measurements described in Sec. IIA was also employed for the present measurements. Since the intermediate state in the desired correlation possesses spin $\frac{1}{2}$, this measurement is equivalent to that of the angular distribution of the Ne^{23} $3.22 \rightarrow 1.02$ transition (i.e., supposedly that measured in the aforementioned gamma-ray angular distribution study). The 2.20-MeV gamma-ray distribution (with respect to the *beam* axis) observed in this study is characterized via Eq. (2) by $a_2/a_0 = -(0.43 \pm 0.04)$ and $a_4/a_0 = +(0.01 \pm 0.03)$: Extreme-angle spectra are depicted in Fig. 10.

The results of the direct 2.20-MeV gamma-ray angular distribution and the 2.20-MeV, 1.02-MeV gamma-ray angular correlation determinations are in good accord. Since both illustrate prominent and self-consistent anisotropic distributions for the 2.20-MeV radiation originating from the 3.22-MeV Ne^{23} state, it is readily ascertained that $J = \frac{1}{2}$ for the 3.22-MeV Ne^{23} state is ruled against with $>99.9\%$ statistical

confidence. Therefore, a $J^\pi = \frac{3}{2}^-$ assignment to the 3.22-MeV Ne^{23} state is established by combining the determination of Pullen, Sperduto, and Kashy² with the present results.

III. SUMMARY OF SPECTROSCOPIC DATA

Presently available spectroscopic information on Ne^{23} states below 4-MeV excitation energy is summarized in Fig. 11, Table I, and Table III. Since the spin of the Ne^{23} ground state is of particular importance as regards the interpretation of the angular correlation measurements as described in Sec. IIB, presently available data on this particular state are considered in detail below. Further discussions concerning information on the relevant excited states of Ne^{23} are also presented in this section.

A. The Ne^{23} Ground State

Several angular distribution measurements on the $\text{Ne}^{22}(d, p)\text{Ne}^{23}$ ground-state proton group have been reported, and all of these studies have indicated $l_n = 2$ and hence $J^\pi = \frac{3}{2}^+$ or $\frac{5}{2}^+$ for this state.^{2,12,13} Evidence that the Ne^{23} ground state is most probably $\frac{5}{2}^+$ is summarized as follows: (1) The $(1.78 \pm 0.10) \times 10^{-10}$ sec half-life determined by Fossan, McDonald, and Chase⁴ for gamma de-excitation of the $\frac{1}{2}^+$, 1.02-MeV first excited state of Ne^{23} is most consistent for an essentially pure electric quadrupole transition ($|M(E2)|^2 = 1.0 \pm 0.1$, $|M(M1)|^2 = (1.6 \pm 0.2) \times 10^{-4}$, where $M(\sigma\lambda)$ denotes the Weisskopf matrix element for a type σ and

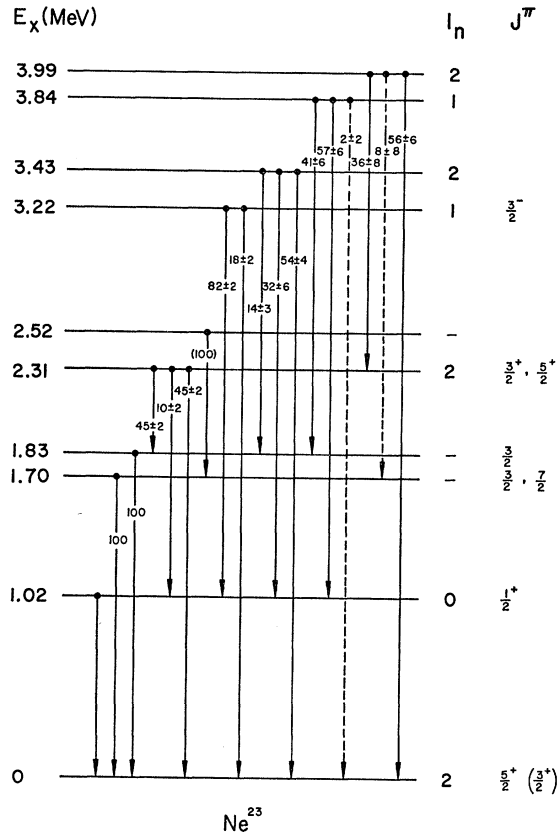


FIG. 11. Energy-level diagram for Ne^{23} . The excitation energy, neutron orbital momentum transfer, and parity values are those reported in Ref. 2; spin assignments are those deduced from Ref. 2 and the present work, and the branching ratios are those determined in the present studies.

multipolarity λ transition¹⁷) and hence is in good accord with $J^\pi = \frac{5}{2}^+$ for the Ne^{23} ground state; (2) The value $\log ft = 6.4 \pm 0.1$ measured by Penning and Schmidt¹⁸ for the beta transition from the Ne^{23} ground state to the 2.08-MeV Na^{23} level, for which $J^\pi = \frac{7}{2}^+$ is highly probable,¹⁹ disfavors $J^\pi = \frac{3}{2}^+$ [i.e., $\Delta J = 2$ (no)] as compared to $J^\pi = \frac{5}{2}^+$ [i.e., $\Delta J = 1$ (no)] for the Ne^{23} ground state; (3) systematics of other odd nucleon count $Z = 13$ nuclear structures (i.e., Mg^{25} , Al^{25} , Al^{27}) imply $J^\pi = \frac{5}{2}^+$ for the Ne^{23} ground state, and, more generally, well-studied adjacent odd- A nuclear systems characteristically possess a single low-lying ($E_x \leq 0.5$ MeV) state for which prominent $l = 2$ stripping behavior in relevant (d, p) or (d, n) reactions and for which additionally $J = \frac{5}{2}$ have been firmly established.^{8, 20}

The above evidence appears sufficiently indicative to warrant the assumption that $J^\pi = \frac{5}{2}^+$ for the Ne^{23}

ground state, and this assumption was therefore incorporated in the correlation analyses presented in Sec. IIB. It is emphasized that the $J^\pi = \frac{3}{2}^+$ possibility for the Ne^{23} ground state has not been *rigorously* eliminated by previously reported measurements and could not be eliminated on the basis of the present measurements; the correctness of the spin assignments or limitations thereon for the 1.70-, 1.83-, and 2.31-MeV states as presented herein is dependent upon the fact that J is $\frac{5}{2}$ for the Ne^{23} ground state.

B. Excited States in Ne^{23}

Concerning the 1.02-MeV state, $l_n = 0$ stripping characteristics have been observed in the formation of this state via the $\text{Ne}^{22}(d, p)\text{Ne}^{23}$ reaction,^{2, 12, 13} and so $J^\pi = \frac{1}{2}^+$ has been firmly established for this state. The present studies show that each of the two proton-gamma correlation measurements involving the 1.02-MeV state appear isotropic within 1.8 and 1.2% statistics, respectively, and hence are consistent with $J = \frac{1}{2}$ for this state.

As concerns each of the 1.70- and 1.83-MeV Ne^{23} states, stripping behavior has not been observed in the formation of these states via the $\text{Ne}^{22}(d, p)\text{Ne}^{23}$ reaction.² The only de-excitation transitions originating from each of these states as observed in either the $\text{Na}^{23}(n, p\gamma)\text{Ne}^{23}$ measurements of Bass and Saleh³ or the present $\text{Ne}^{22}(d, p\gamma)\text{Ne}^{23}$ studies were the respective gamma rays to the ground state. It has been concluded in Sec. IIB that $J = \frac{3}{2}$ or $\frac{7}{2}$ for the 1.70-MeV state and that $J = \frac{3}{2}$ for the 1.83-MeV state.

The limitation $J^\pi = \frac{3}{2}^+$ or $\frac{5}{2}^+$ for the 2.31-MeV Na^{23} state has been indicated by the proton angular distribution measurements of Pullen, Sperduto, and Kashy.² The present angular-correlation studies involving the de-excitation gamma rays originating from this state do not establish a meaningful preference between these two possibilities. While the gamma-ray branching ratios associated with this state as observed in the measurements of Bass and Saleh on the $\text{Na}^{23}(n, p\gamma)\text{Ne}^{23}$ reaction³ [i.e., $\sim (55 \pm 30)\%$, $< 15\%$, $< 15\%$, and $\sim (45 \pm 30)\%$ relative intensities to the respective 1.83-, 1.70-, 1.02-, and 0-MeV Ne^{23} states] are in acceptable accord with the present results given in Table I and Fig. 11, the relatively large experimental uncertainties in the former determination concerning this state preclude a precise intercomparison of the two results.

As regards the 2.52-MeV Ne^{23} state, previous $\text{Ne}^{22}(d, p)\text{Ne}^{23}$ particle angular distribution measurements have not indicated stripping characteristics in its formation.² Gamma-ray branching ratios associated with this state have been determined in the $\text{Na}^{23}(n, p\gamma)\text{Ne}^{23}$ measurements of Bass and Saleh³ with considerably greater precision than was obtained in the present measurements. Their results³ indicate that the 2.52-MeV state de-excites with $< 4\%$, $(80 \pm 6)\%$,

¹⁷ D. H. Wilkinson, in *Nuclear Spectroscopy*, edited by F. Ajzenberg-Selove (Academic Press Inc., New York, 1960), Chap. V. F.

¹⁸ J. R. Penning and F. H. Schmidt, *Phys. Rev.* **105**, 647 (1957).

¹⁹ A. R. Poletti and D. F. H. Start, *Phys. Rev.* **147**, 800 (1966).

²⁰ P. M. Endt and C. Van der Leun, *Nucl. Phys.* **34**, 1 (1962).

$<4\%$, and $(20\pm 6)\%$ relative intensities to the respective 1.83-, 1.70-, 1.02-, and 0-MeV states; the relevant entries in Table I show that the present results are in accord with the above determinations.

The 3.22- and 3.84-MeV Ne^{23} states have each been observed to display $l_n=1$ stripping characteristics in their formation via the $\text{Ne}^{22}(d, p)\text{Ne}^{23}$ reaction,² and consequently possible assignments $J^\pi=\frac{1}{2}^-$ or $\frac{3}{2}^-$ have been indicated for each of these two states. The 3.22-MeV state has been found to de-excite predominantly to the 1.02-MeV state, and gamma-ray correlation measurements reported in Sec. IIC establish $J\geq\frac{3}{2}$ for this state; consequently, $J^\pi=\frac{3}{2}^-$ for the 3.22-MeV state. With regard to the 3.84-MeV state, the presently reported gamma-ray branching ratio observations associated with this level [i.e., $(41\pm 6)\%$, $(57\pm 6)\%$, and $\leq 4\%$ relative intensities for transitions to the 1.83-, 1.02-, and 0-MeV Ne^{23} states, respectively] indicate at least a pronounced relative inhibition or perhaps an essential absence of the de-excitation mode to the Ne^{23} ground state. When compared with the situation in the relatively well-studied Mg^{25} and Al^{25} nuclear systems with respect to low-lying negative parity states,²⁰ the present evidence suggests that the $J^\pi=\frac{1}{2}^-$ assignment to the 3.84-MeV Ne^{23} state is to be tentatively preferred to the $\frac{3}{2}^-$ possibility.

Finally, both of the 3.43- and 3.99-MeV Ne^{23} states have displayed $l_n=2$ stripping characteristics in their formation via the $\text{Ne}^{22}(d, p)\text{Ne}^{23}$ reaction²; the present studies establish only the gamma-ray branching ratios associated with each of these two states.

IV. COLLECTIVE ASPECTS OF LOW-LYING STATES IN Ne^{23}

A. Orientation

The successful interpretation of many of the properties associated with odd- A nuclear systems immediately adjacent to Ne^{23} , such as Ne^{21} - Na^{21} , Na^{23} , and Mg^{25} - Al^{25} , via the Nilsson strong-coupling collective model²¹ is established to the point that a similar description applied to the properties of Ne^{23} is expected to be in similar agreement with the relevant observations.^{1,22-25} Since the behavior of the unpaired nucleon in an odd A nuclear configuration is of pronounced importance in the framework of the strong coupling collective model representation of nuclear structure, rotational band structures in Mg^{25} - Al^{25} and Ne^{23} are anticipated to be similar, all three nuclei being odd-nucleon count $\zeta=13$ systems. Additionally, the model-predicted²¹ level sequence and spacing in a given system ultimately

²¹ S. G. Nilsson, Kgl. Danske Videnskab. Selskab, Mat. Fys. Medd. **29**, No. 16 (1955).

²² A. E. Litherland, H. McManus, E. B. Paul, D. A. Bromley, and H. E. Gove, Can. J. Phys. **36**, 378 (1958).

²³ R. M. Drezler, Phys. Rev. **132**, 1166 (1963).

²⁴ W. Glöcke, Z. Physik **178**, 53 (1964).

²⁵ A. J. Howard, J. P. Allen, and D. A. Bromley, Phys. Rev. **139**, 1135 (1965).

depends most strongly on the moment of inertia parameter, $\hbar^2/2I$, and the spin-orbit coupling-strength parameter, κ . Present evidence delimits $\hbar^2/2I$ to $+(0.19\pm 0.03)$ MeV for Ne^{22} (the model core configuration for Ne^{23}) and $+(0.21\pm 0.02)$ for Mg^{24} (the model core configuration for Mg^{25} - Al^{25}) and also indicates that κ is slowly varying in this mass region.²⁶ Therefore, a *marked* similarity between Ne^{23} and Mg^{25} - Al^{25} system properties is predicted by basic model considerations, and it is of interest to attempt a preliminary comparison involving the observations on Ne^{23} , the information on Mg^{25} - Al^{25} , and the $\zeta=13$ strong-coupling collective-model predictions.

Detailed calculations^{22,26,27} applied to the Mg^{25} - Al^{25} nuclear systems have strongly implied a prolate deformation, parameterized by $\eta\approx+4$, and have further indicated that inclusion of the $K^\pi=\frac{5}{2}^+$, $\frac{1}{2}^+$, $\frac{1}{2}^+$, and $\frac{1}{2}^-$ rotational bands associated with location of the extra-core nucleon in Nilsson orbit 5, 9, 11, and 14, respectively, results in a notably successful interpretation concerning not only the static but also the dynamic properties of Mg^{25} - Al^{25} states below ~ 4 -MeV excitation energy. Within the model framework, configuration mixing to first order is attributed to the Coriolis interaction existent between states of identical spin and parity which are members of rotational bands with $|\Delta K|\leq 1$, and so, in the above considerations concerning Mg^{25} - Al^{25} , only members of the two $K^\pi=\frac{1}{2}^+$ rotational bands based upon Nilsson orbits 9 and 11 are predicted to be displaced significantly from their unperturbed (pure) model-predicted energies. Relatedly, dipole gamma-ray transitions between two unmixed rotational band states with $|\Delta K|\geq 2$ are model-forbidden to first order.

B. Results for Ne^{23}

Although presently available information concerning the properties of the Ne^{23} nuclear system remains relatively limited, it appears to be sufficient to establish

TABLE IV. Tentative Nilsson-model rotational-band-member assignments to low-lying Ne^{23} states.

Observed state (MeV)	Band ^a	K	π	J
0	5	$\frac{5}{2}$	+	$\frac{5}{2}$
1.02	9	$\frac{1}{2}$	+	$\frac{1}{2}$
1.70	5	$\frac{5}{2}$	+	$\frac{7}{2}$
1.83	9	$\frac{1}{2}$	+	$\frac{3}{2}$
2.31	9	$\frac{1}{2}$	+	$\frac{5}{2}$
2.52	5	$\frac{5}{2}$	+	$\frac{9}{2}$
3.22	14	$\frac{1}{2}$	-	$\frac{3}{2}$
3.43	11	$\frac{1}{2}$	+	$\frac{3}{2}$
3.84	14	$\frac{1}{2}$	-	$\frac{1}{2}$
3.99	11	$\frac{1}{2}$	+	$\frac{5}{2}$

^a Tabulated numbers correspond to the Nilsson orbit numbers.

²⁶ I. Kelson and C. A. Levinson, Phys. Rev. **134**, B269 (1964).

²⁷ W. Scholz and F. B. Malik (private communication).

TABLE V. Ratios of cascade to ground-state reduced gamma-ray transition widths in Ne^{23} for assumed dipole transitions.^a

E_f (MeV)	1.70	1.83	2.31	E_i (MeV) 2.52	3.22	3.43	3.84	3.99
1.02	<i><0.82</i>	<i><0.61</i>	<i>1.3±0.3</i>	...	14±2	<i>1.7±0.5</i>	<i>>32</i>	...
1.70	<i>130±40</i>
1.83	110±10	<i>2.5±0.7</i>	<i>>62</i>	...
2.31	9±3

^a Tabulated values in italics denote situations where a dipole transition for one of the two relevant transitions may be disallowed by the angular-momentum selection rule (see Fig. 11).

a semiquantitatively correct Nilsson model representation of the ten established Ne^{23} states below an excitation energy of 4 MeV. The *predominant* Nilsson-model pure configuration assignment to each of these ten states which is suggested by the comparisons presented in the ensuing subsections is summarized in Table IV.

1. Members of Nilsson Orbit 5

Accepting $J^\pi = \frac{5}{2}^+$ for the Ne^{23} ground state (as discussed in Sec. IIIA), a Nilsson Orbit 5, $K^\pi J = \frac{5}{2}^+ \frac{5}{2}$ assignment follows, analogous to the Mg^{25} - Al^{25} ground-state situation.²² It is therefore anticipated that dipole transitions originating from members of the three $K = \frac{1}{2}$ rotational bands, which will account for seven of the remaining nine Ne^{23} states under discussion, and terminating at the Ne^{23} ground state, should be relatively inhibited (forbidden to first order). Employing the data summarized in Sec. III and Fig. 11, relative inhibition factors for transitions to the Ne^{23} ground state have been determined by calculating for each state the ratio of the reduced transition width¹⁷ for each observed cascade radiation to the reduced transition width for the observed ground-state radiation. Pure dipole transitions have been assumed in this calculation, the results of which are presented in Table V. The six entries in italics in Table V represent situations wherein a *dipole* transition for one of the two radiations may possibly be disallowed by the dipole transition selection rule, $|\Delta J| \leq 1$. Tentative spin identifications as presented in Table IV indeed would preclude dipole radiation for one of the transitions in each of these six cases. Confining attention to the five unitalicized entries in Table V for which all (ten) transitions involved satisfy the $|\Delta J| \leq 1$ selection rule (see Fig. 11), the average relative ground-state dipole transition inhibition factor obtained from these five cases is ~ 25 , with individual values displaying large scatter from this average. This result is consistent with similar findings concerning the Mg^{25} - Al^{25} system.²²

The present evidence suggests that the $J = \frac{7}{2}$ member of this rotational band is to be identified with the 1.70-MeV Ne^{23} state. The observed gamma-ray branching ratio as well as the measured (lower) magnitude and phase of the multipole amplitude ratio for the $1.70 \rightarrow 0$ transition are in good accord with the model-predicted values for a $J = \frac{7}{2}$ assignment to the 1.70-MeV state. It

is also noted that in all cases wherein there is an absence of detected radiations originating from the higher lying states (considered below) to the 1.70-MeV state, violation of one or both of the dipole gamma-ray transition selection rules $|\Delta J| \leq 1$, $|\Delta K| \leq 1$ is indicated for said model transition. Finally, the excitation energies of assigned Nilsson orbit 5, $K^\pi J = \frac{5}{2}^+ \frac{7}{2}$ states in Ne^{23} , Mg^{25} , and Al^{25} are comparable, being 1.70, 1.61, and 1.61 MeV, respectively. Identification of the $J = \frac{9}{2}$ member of this rotational band is comparatively speculative: Present evidence suggests, however, that the properties observed for the 2.52-MeV Ne^{23} state are most reasonably interpreted via a Nilsson orbit 5, $K^\pi J = \frac{5}{2}^+ \frac{9}{2}$ assignment thereto.

2. Members of Nilsson Orbit 9

The experimental observations on Ne^{23} states below 4-MeV excitation energy indicate that the 1.02-, 1.83-, and 2.31-MeV states are successfully interpretable as being predominantly the respective $J = \frac{1}{2}, \frac{3}{2}, \frac{5}{2}$ members of the Nilsson-orbit-9, $K^\pi = \frac{1}{2}^+$ rotational band. The observed lifetime of the 1.02-MeV state,⁴ characterized by $|M(E2)|^2 = 1.0 \pm 0.1$, is in accord with model-predictions for an (unenhanced) interband $E2$ transition, and the Nilsson-Orbit-9, $K^\pi J = \frac{1}{2}^+ \frac{1}{2}$ assignment to the 1.02-MeV Ne^{23} state appears as well-established as the corresponding assignment to the 0.58- and 0.45-MeV states in Mg^{25} and Al^{25} , respectively.

The situation regarding the 1.83-MeV state is more problematic. The absence of stripping² characteristics in its formation via the $\text{Ne}^{22}(d,p)\text{Ne}^{23}$ reaction and the weak cascade de-excitation to the 1.02-MeV state are in disagreement with expectations deduced from relevant model considerations on the Mg^{25} - Al^{25} system. Indeed, the relative ground-state dipole transition inhibition factor of <0.62 computed for this Ne^{23} case represents one of the outstanding discrepancies deduced in the present intercomparison (the relevant inhibition factors in Mg^{25} and Al^{25} are 14.1 and 9.5, respectively²²). Nonetheless, a predominant Nilsson-orbit-9, $K^\pi J = \frac{1}{2}^+ \frac{3}{2}$ assignment to the 1.83-MeV Ne^{23} state appears to be the most tenable choice at the present time.

The observed properties associated with the formation and decay of the 2.31-MeV state are in qualitative correspondence with those associated with the 1.96- and 1.81-MeV states in Mg^{25} and Al^{25} , which have been

successfully interpreted²² as predominantly Nilsson-orbit-9, $K^\pi J = \frac{1}{2}^+ \frac{5}{2}$ members. Consequently, a similar model assignment is indicated for the 2.31-MeV Ne^{23} state.

3. Members of Nilsson Orbit 14

The lack of participation (to first order) in configuration mixing between appropriate members of either the $K^\pi = \frac{5}{2}^+$ or the $K^\pi = \frac{1}{2}^-$ rotational bands based on Nilsson orbits 5 and 14, respectively, with members of the other two bands under consideration results in the model prediction that the excitation energy associated with the Nilsson orbit 14 rotational band-head should be essentially the same in Ne^{23} , Mg^{25} , and Al^{25} . In the mass-25 system, members of a distorted Nilsson orbit 14, $K^\pi = \frac{1}{2}^-$ rotational band have been assigned as follows:²² $J = \frac{3}{2}, \frac{7}{2},$ and $\frac{1}{2}$ to the respective 3.40-, 3.97-, and 4.26-MeV Mg^{25} states and to the respective 3.09-, 3.72-, and 3.85-MeV Al^{25} states. It follows that a Nilsson-orbit-14, $K^\pi J = \frac{1}{2}^- \frac{3}{2}$ assignment to the 3.22-MeV Ne^{23} state appears as well-established as that in the above-discussed mass-25 situation; the present comparison also indicates the tentative $K^\pi J = \frac{1}{2}^- \frac{1}{2}$ assignment to the 3.84-MeV Ne^{23} state as consistent. The apparent absence in Ne^{23} of a $\frac{7}{2}^-$ state intermediate in energy between the two negative parity states just discussed is not considered at present to be a serious discrepancy when compared to the mass-25 situation. A modest variation of the decoupling parameter²¹ associated with this $K = \frac{1}{2}$ rotational band is sufficient to place the $\frac{7}{2}$ member above the $\frac{1}{2}$ member and hence to promote it into the region above 4-MeV excitation energy, where possible candidates for such a state presently exist.

4. Members of Nilsson Orbit 11

In attempting to continue the comparison as concerns Nilsson orbit 11, $K^\pi = \frac{1}{2}^+$ rotational band members, it is apparent that the information concerning the 3.43- and 3.99-MeV Ne^{23} states is consistent with predominant Nilsson orbit 11, $K^\pi J = \frac{1}{2}^+ \frac{3}{2}$ and $\frac{1}{2}^+ \frac{5}{2}$ assignments to these states, more consistent in the presented order. However, a second outstanding discrepancy between

observed and model-predicted results for Ne^{23} is the apparent absence in the observed Ne^{23} energy spectrum of the model-predicted $J = \frac{1}{2}$ member of the Nilsson orbit 11 rotational band. This discrepancy is emphasized by the fact that Nilsson orbit 11 $K^\pi J = \frac{1}{2}^+ \frac{1}{2}, \frac{1}{2}^+ \frac{3}{2},$ and $\frac{1}{2}^+ \frac{5}{2}$ assignments have been given to the respective 2.56-, 2.80-, and 3.90-MeV Mg^{25} states and also to the respective 2.50-, 2.70-, and 3.88-MeV Al^{25} states.²² Thus the situation regarding Ne^{23} states interpretable as predominant Nilsson orbit 11 members is especially ambiguous at the present time.

C. Summary

The observed properties of the ten presently known Ne^{23} states below 4-MeV excitation energy have been found to be consistent with a Nilsson model representation which is primarily anticipated from mass-25 results.²² Two notable discrepancies have been enunciated: (1) The observed and model-predicted formation and decay properties associated with the 1.83-MeV Ne^{23} state are significantly at variance with one another; (2) that which arises from the absence, in the experimental spectrum, of the second $J^\pi = \frac{1}{2}^+$ state predicted below ~ 4 -MeV excitation energy by the model. It is clear that further angular-correlation and absolute-lifetime measurements, involving states of Ne^{23} below 4-MeV excitation energy, are necessary in order to permit a more thorough investigation of the apparent collective behavior displayed in the Ne^{23} nuclear structure.

ACKNOWLEDGMENTS

We are grateful to Dr. W. W. Watson for his contribution in connection with the gaseous target material employed in the present studies. We are also indebted to Dr. D. J. Pullen and Dr. R. Bass for valuable communications concerning their works prior to publication. A. J. Howard, J. P. Allen, and D. A. Bromley again wish to thank Dr. D. E. Alburger for his extensive hospitality at the Brookhaven National Laboratory. The assistance of R. A. Lindgren during these studies is much appreciated.